International Journal of Pharmaceutics 495 (2015) 312–317

Contents lists available at ScienceDirect

International Journal of Pharmaceutics

journal homepage: www.elsevier.com/locate/ijpharm

Physical stability of drugs after storage above and below the glass transition temperature: Relationship to glass-forming ability

Amjad Alhalaweh[a,*], Ahmad Alzghoul[b], Denny Mahlin[a], Christel A.S. Bergström[a]

[a] Department of Pharmacy, Uppsala University, Uppsala Biomedical Centre, P.O. Box 580, SE-751 23 Uppsala, Sweden
[b] Department of Information Technology, Uppsala University, Lägerhyddsv. 2, hus 1, Box 337, SE- 751 05 Uppsala, Sweden

ARTICLE INFO

Article history:
Received 3 July 2015
Received in revised form 28 August 2015
Accepted 29 August 2015
Available online 1 September 2015

Keywords:
Amorphous
Physical stability
Glass-forming ability
SVM
Computational prediction

ABSTRACT

Amorphous materials are inherently unstable and tend to crystallize upon storage. In this study, we investigated the extent to which the physical stability and inherent crystallization tendency of drugs are related to their glass-forming ability (GFA), the glass transition temperature (T_g) and thermodynamic factors. Differential scanning calorimetry was used to produce the amorphous state of 52 drugs [18 compounds crystallized upon heating (Class II) and 34 remained in the amorphous state (Class III)] and to perform in situ storage for the amorphous material for 12 h at temperatures 20 °C above or below the T_g. A computational model based on the support vector machine (SVM) algorithm was developed to predict the structure-property relationships. All drugs maintained their Class when stored at 20 °C below the T_g. Fourteen of the Class II compounds crystallized when stored above the T_g whereas all except one of the Class III compounds remained amorphous. These results were only related to the glass-forming ability and no relationship to e.g. thermodynamic factors was found. The experimental data were used for computational modeling and a classification model was developed that correctly predicted the physical stability above the T_g. The use of a large dataset revealed that molecular features related to aromaticity and π–π interactions reduce the inherent physical stability of amorphous drugs.

1. Introduction

Drugs that are in an amorphous state have significantly different properties from those of their crystalline counterparts. When poorly soluble drugs are in an amorphous state, they have a higher dissolution rate and are more soluble (Hancock et al., 2002; Hancock and Parks, 2000; Marsac et al., 2006a). There has been increasing interest in incorporating poorly soluble drugs in medicinal products in their amorphous form, in order to improve their absorption, and hence their bioavailability. However, amorphous materials are not stable and their tendency to crystallize is a challenge when formulations of the amorphous form of the drug are being developed (Hancock et al., 1995; Yoshioka et al., 1994; Yu, 2001). Research efforts have been directed towards improved understanding of the driving force for crystallization in these materials and the conditions that might prolong their physical stability (Andronis and Zografi, 1998; Hancock et al., 1995, 1998; Kauzmann, 1948; Yoshioka et al., 1994). It has been estimated that the amorphous state can be kinetically stable if it is stored at a temperature well below the glass transition temperature (T_g) (Andronis and Zografi, 1998; Hancock et al., 1995; Kauzmann, 1948). The T_g is an intrinsic property of amorphous materials and is therefore often used to indicate their physical stability (Angell, 1988). The physical properties of the materials above and below the T_g are different and reflect the physical stability of the material (Andronis and Zografi, 1998; Graeser et al., 2009; Hancock et al., 1995; Yoshioka et al., 1994). The material is considered to exist in a glassy (solid) state below the T_g and as a supercooled liquid above the T_g. Currently, the mechanistic understanding of the driving force for crystallization above and below the T_g is sparse and studies of the chemical modifications or formulation strategies that might result in improved performance of amorphous solid dosage forms are warranted.

The stability of amorphous materials upon storage above and below the T_g has been investigated in several studies, but in each of these only a limited number of compounds has been included (Andronis and Zografi, 1998; Graeser et al., 2009; Hancock et al., 1995; Yoshioka et al., 1994). These studies linked the crystallization process to molecular mobility, which increases at higher

* Corresponding author. Fax: +46 18 471 4223.
E-mail address: amjad.alhalaweh@farmaci.uu.se (A. Alhalaweh).

http://dx.doi.org/10.1016/j.ijpharm.2015.08.101
0378-5173/

temperatures and hence is higher above the T_g. Thus, materials have a higher tendency to crystallize above than below the T_g. Other studies have found that molecular mobility is not predictive enough to be used as the only determinant for stability in the amorphous state and that other factors such as the configurational entropy(Zhou et al., 2002) and enthalpy (Marsac et al., 2006b) have significant impact on the stability (Graeser et al., 2009; Hancock et al., 1998).

In the area of material science, the stability of the amorphous state has been defined as the resistance of glasses to devitrification upon reheating (especially near or somewhat above the T_g) (Weinberg, 1994). The relationship between glass stability (GS) and glass-forming ability (GFA) has been explored, but only modest relationships have been reported (Baird et al., 2010; Mahlin and Bergström, 2013; Mahlin et al., 2011; Nascimento et al., 2005). However, a classification system based on the GFA of drug compounds has recently been presented and this system has been related to the GS of the compounds (Baird et al., 2010; Mahlin and Bergström, 2013; Mahlin et al., 2011). In these studies, the crystallization tendency scheme designed by Taylor and coworkers was used (Baird et al., 2010). They divided compounds into three classes, depending on how easily the compounds crystallized during a heat-cool-heat cycle. Class I compounds are defined as those that crystallize upon cooling the melt, whereas Class II and Class III compounds form an amorphous material upon cooling the melt. Class II and III compounds are differentiated in that Class II

Table 1
Compounds used in the study with their molecular weight (MW), melting temperature (T_m), heat of fusion (ΔH), glass transition temperature (T_g), temperature for the stability test above T_g ($T_{above} = T_g + 20$), change in free energy (ΔG) between the supercooled liquid and the crystalline state at T, and result of the stability test (no = crystalline and yes = amorphous). Pi_AQc = sum of absolute values of Hückel pi atomic charges on C atoms; F_AromB = number of aromatic bonds as a fraction of total bonds; TR = training set; TS = test set.

Compound	Class	MW (g/mole)	T_m (K)	ΔH kJ/mole	T_g (K)	T_{above} (K)	T_g/T_{above}	ΔG (kJ/mol)	Stable above T_g[a]	Pi_AQc	F_AromB	TR/TS
Acetaminophen	II	151.2	443	29	299	319	0.94	5.9	No	0.48	0.55	TR
Celecoxib	II	318.4	436	32	331	351	0.94	5.1	No	0.45	0.61	TR
Danazol	II	337.5	500	36	352	372	0.95	6.8	No	0.15	0.17	TR
Estradiol	II	22.4	451	2	358	378	0.95	0.3	No	0.22	0.26	TR
Nifedipine	II	346.3	446	39	320	340	0.94	7.0	No	1.00	0.23	TR
Orlistat	II	495.8	316	56	228	248	0.92	9.4	No	0.72	0	TR
Pimozide	II	461.6	492	50	335	355	0.94	10.1	No	0.53	0.58	TR
Tamoxifen	II	371.5	371	56	263	283	0.93	10.2	Yes	0.24	0.60	TR
Tenofovir	II	28.2	552	3	416	436	0.95	1.2	No	0.29	0.50	TR
Testosterone	II	288.4	426	26	315	335	0.94	4.4	No	0.40	0	TR
Tinidazole	II	247.3	289	36	266	286	0.93	0.4	No	0.20	0.31	TR
Tolazamide	II	311.4	445	41	297	317	0.94	8.3	Yes	0.40	0.27	TR
Aripiprazole	II	448.4	517	48	363	383	0.95	9.2	No	0.94	0.36	TS
Bicalutamide	II	430.4	465	51	323	343	0.94	9.9	No	0.82	0.40	TS
Cinnarizine	II	368.5	394	43	280	300	0.93	7.7	Yes	0.03	0.58	TS
Clemastine	II	343.9	451	48	308	328	0.94	9.6	No	0.09	0.46	TS
Fluorescamine	II	278.3	426	28	299	319	0.94	5.7	Yes	0.83	0.50	TS
Flurbiprofen	II	244.3	388	28	270	290	0.93	5.4	No	0.38	0.63	TS
Acemetacin	III	415.8	421	48	310	330	0.94	8.1	Yes	1.34	0.52	TR
Budesonide	III	430.5	530	39	368	388	0.95	7.6	Yes	0.73	0	TR
Captopril	III	217.3	380	29	277	297	0.93	4.9	Yes	0.46	0	TR
Carvedilol	III	406.5	390	53	315	335	0.94	6.4	Yes	0.83	0.64	TR
Chloramphenicol	III	323.1	425	4	304	324	0.94	0.7	Yes	0.39	0.30	TR
Chlorhexidine	III	505.5	408	43	336	356	0.94	4.7	Yes	0.86	0.34	TR
Clotrimazole	III	344.9	418	35	303	323	0.94	6.1	Yes	0.29	0.82	TR
Emtricitabine	III	247.2	426	27	344	364	0.95	3.4	No	0.41	0.35	TR
Ezetimibe	III	409.4	437	40	338	358	0.94	6.0	Yes	0.74	0.55	TR
Felodipine	III	384.3	420	34	318	338	0.94	5.3	Yes	0.93	0.23	TR
Hydrocortisone	III	362.5	497	45	359	379	0.95	8.1	Yes	0.69	0	TR
Ibuprofen[b]	III	206.3	350	27	228	248	0.92	5.5	Yes	0.30	0.40	TR
Indomethacin	III	356.7	434	42	318	338	0.94	7.2	Yes	1.10	0.59	TR
Itraconazole	III	705.7	441	65	331	351	0.94	10.6	Yes	1.02	0.51	TR
Ketoprofen	III	254.3	368	31	270	290	0.93	5.2	Yes	0.72	0.60	TR
Linaprazan	III	366.5	519	55	373	393	0.95	10.1	Yes	0.73	0.55	TR
Metolazone	III	365.8	539	36	382	402	0.95	6.8	Yes	0.87	0.46	TR
Nizatidine	III	331.5	406	45	286	306	0.93	8.4	Yes	0.50	0.24	TR
Physostigmine	III	275.4	377	32	293	313	0.94	4.5	Yes	0.47	0.27	TR
Simvastatin	III	418.8	412	29	309	329	0.94	4.6	Yes	0.51	0	TR
Spironolactone	III	416.6	486	24	364	384	0.95	4.0	Yes	0.90	0	TR
Sulindac	III	356.4	460	32	348	368	0.95	5.2	Yes	0.74	0.44	TR
Zolmitriptan	III	287.4	410	34	322	342	0.94	4.7	Yes	0.56	0.43	TR
Bucindolol	III	363.5	459	38	356	376	0.95	5.6	Yes	0.79	0.55	TS
Fenofibrate[b]	III	360.8	354	35	256	276	0.93	6.1	Yes	0.91	0.46	TS
Glafenine	III	372.8	437	43	337	357	0.94	6.4	Yes	0.90	0.61	TS
Glibenclamide	III	494	445	51	333	353	0.94	8.3	Yes	0.81	0.34	TS
Hydrochlorothiazide	III	297.7	536	34	391	411	0.95	6.1	Yes	0.61	0.33	TS
Hydroflumethiazide	III	297.9	542	39	373	393	0.95	7.9	Yes	0.48	0.29	TS
Isradipine	III	371.4	432	34	316	336	0.94	5.8	Yes	0.86	0.34	TS
Ketoconazole	III	531.4	423	54	318	338	0.94	8.7	Yes	0.90	0.43	TS
Nandrolone	III	274.4	397	21	310	330	0.94	2.9	Yes	0.41	0	TS
Nimesulide[b]	III	308.3	423	36	296	316	0.94	6.7	Yes	0.43	0.55	TS
Warfarin	III	308.3	435	45	345	365	0.95	6.0	Yes	1.03	0.68	TS

[a] No = not amorphous after the stability study; yes = amorphous after the stability study.
[b] Behaved like a Class II drug after the stability study.

compounds crystallize upon heating the amorphous material, whereas Class III compounds remain amorphous (Baird et al., 2010; Mahlin and Bergström, 2013). The physical stability of the amorphous form of a drug has been related to thermodynamic factors, and factors such as viscosity and the entropy difference between the melt and the undercooled liquid have been suggested to be driving forces for crystallization (Bhugra and Pikal, 2008; Kawakami et al., 2014; Trasi et al., 2014). However, the thermodynamic properties are difficult to assess below the T_g and have only been related to physical stability above the T_g for a limited number of compounds (Graeser et al., 2009).

This work investigated the relationships between the physical stability above and below the T_g under dry conditions to gain a better understanding of the deviations existing in the relation between storage stability and T_g. A large number of drug compounds were studied to provide a mechanistic understanding of the driving forces behind crystallization. The relationship between the T_g and the physical stability, and the change in free energy (ΔG_v) between the melt and the crystalline state and the physical stability after storage was investigated. Further, computational models that predict the physical stability of compounds from their molecular structure were developed to better understand the molecular properties that are important for glass stability.

2. Methods

2.1. Materials

All chemicals were of high purity (98.0–99.9%) and purchased from Sigma–Aldrich (Stockholm, Sweden) except for danazol (Coral drugs IVT, India), itraconazole (Lee Pharma Ltd., India) ezetimibe and ketoconazole (TCR, Toronto, Canada) and bicalutamide, felodipine and linaprazan which were received as a kind gift from AstraZeneca (Mölndal, Sweden), The compounds were selected to provide a wide range of T_gs (225–425 K; Table 1) and all were previously identified as compounds with GFA (Alhalaweh et al., 2014).

2.2. Production of the amorphous state

The amorphization of each compound was performed by in situ quenching in a differential scanning calorimetry (DSC) Q2000 (TA) instrument calibrated for temperature and enthalpy using indium. The instrument was equipped with a refrigerated cooling system. The melting point and heat of fusion were determined for each compound using an amount of 1–3 mg in non-hermetic aluminium pans. The compounds were scanned at a heating rate of 10 °C/min under a continuously purged dry nitrogen atmosphere (50 mL/min).

Glass formation was investigated by weighing 1–3 mg of the compound into a non-hermetic pan and heating to about 2 °C above the peak melting temperature. The system was kept isothermal for 2 min to obtain complete melting and was thereafter cooled to −70 °C at a ramp rate of 20 °C/min. The formation of an amorphous state was then investigated by performing a second heat cycle using a heating rate of 20 °C/min immediately after cooling. The production of an amorphous state was indicated by detection of the T_g upon heating.

2.3. In situ storage in the DSC instrument

After formation of the amorphous materials described in the previous section, an in situ storage study was performed in the DSC instrument. A time frame of 12 h was used and the study was performed twice: 20 °C above and 20 °C below the T_g. The following experimental protocol was used. The sample was:

1. heated to about 2 °C above the peak melting temperature, and was thereafter kept isothermal for 2 min to ensure complete melting, followed by cooling to −70 °C at a ramp rate of 20 °C/min to produce the amorphous material;
2. heated to 20 °C above the T_g at 20 °C/min and then cooled to 40 °C below the T_g at the same heating rate to remove any thermal history;
3. heated to the storage temperature (20 °C above or below the T_g) and held at this temperature for 12 h;
4. cooled to 40 °C below the T_g at 20 °C/min;
5. heated to 20 °C above melting temperature at a ramp rate of 20 °C/min.

The ΔG_v between the liquid and crystalline phases was calculated by the Hoffman equation (Hoffman, 1958):

$$\Delta G_v = \frac{\Delta H_f (T_m - T) T}{T_m^2}$$

where ΔH_f is the heat of fusion of the crystalline material, T_m is the melting temperature, and T is the temperature of storage.

3.1. Model development

The computational model was developed using 52 compounds and their corresponding molecular descriptors. The total number of descriptors was 280 which were calculated with the software ADMET Predictor (SimulationsPlus, CA) using molecules represented as structure-data files (sdf). The dataset was divided into training (35 compounds) and test (17 compounds) sets based on the T_g values and the Class (II or III) of the compounds. A support vector machine (SVM) algorithm was used to build a prediction model, making use of the forward selection procedure. Support vector machine is a supervised learning method which is considered as one of the most successful classification methods (Suykens and Vandewalle, 1999). The SVM algorithm makes a decision boundary that maximizes the margin between two classes. SVMs also take advantage of nonlinear kernels such as polynomial and Gaussian functions to efficiently perform a non-linear classification by mapping the data into a high dimensional space where it can be linearly separated. The model development procedures started by applying a two-sample t-test to the training set for all molecular descriptors ($n = 280$). The variable that achieved the lowest p-value was selected for further investigation. This variable was used with the remaining 279 descriptors, one at a time, as inputs into the SVM model. A five-fold cross-validation method was applied to the training set to assess the performance of the SVM model for each added descriptor. This procedure was repeated until no improvement in the performance of the model was noticed.

The performance of the SVM model changes as the values of the SVM parameters change. A leave-one-out cross-validation (LOOCV) was used to tune the parameters. The LOOCV involved dividing the data into two groups: the training and testing sets. Only one observation is used for testing, and the rest of data are used for training. The process is then repeated for all observations (i.e. all compounds) so that every observation is left out in turn from the model development and tested. In this work, the LOOCV was used to assess the performance of the SVM model when its sigma parameter was changed. The sigma value which achieved the lowest classification error was assigned to the SVM model.

Table 2
Heat capacity change at T_g (ΔC_p) (J g °C^{-1}) for Class II compounds analysed at time 0 and after 12 and 24 h′ storage.

Time (h)	Cinnarizine	Fluorescamine	Tamoxifen	Tolazamide
0	0.57	0.48	0.49	0.55
12	0.54	0.42	0.46	0.22
24	0.33	0.27	–	0.22

3. Results and discussion

This study was carried out to gain a better molecular understanding of the stability of amorphous compounds and, hence, only compounds that had previously been identified as good glass-formers were investigated (Alhalaweh et al., 2014; Alzghoul et al., 2014). However, compounds from both Class II (where recrystallization occurs upon heating) and Class III (where no recrystallization occurs upon heating) were included. The stability of these compounds was studied under standardized conditions with regard to the T_g. A temperature of 20 °C above and below the T_g was selected, based on the reasoning that all compounds should have the same T_g/T and therefore should have similar prerequisites for crystallization (Table 1). The value of T_g/T correlates well with the initiation time for crystallization, so this effect was normalized (Kawakami et al., 2014).

3.2. Physical stability

There was no change in the solid state when the compounds were stored below the T_g. Therefore, the physical stability of the compound below the T_g on the timescale used (12 h) is highly related to the GFA (Alhalaweh et al., 2014; Baird et al., 2010). The general trend for Class II compounds when stored above the T_g was that they rapidly crystallized (Fig. 1). Among the 18 Class II compounds, only four remained amorphous after the challenge of elevated temperature. These were tolazamide, cinnarizine, fluorescamine and tamoxifen. All the other Class II compounds crystallized upon storage, as confirmed by the DSC analysis, as there was no sign of a T_g in the second heating and the enthalpy on melting corresponded to that of the crystalline drug. However, the difference in heat capacity change at the T_g (ΔC_p) for the four stable compounds was lower after storage than at time zero (Table 2). This suggested that the compounds might crystallize upon long term storage and we therefore extended the stability study to 24 h for these substances. After the additional 12 h at the elevated temperature, tamoxifen crystallized and the remaining compounds remained amorphous with further reduced ΔC_p values (Table 2).

The results for the stability of the Class III compounds are presented in Fig. 2. Thirty-three of the 34 compounds (97%) remained amorphous after storage, with emtricitabine the only exception. Although a T_g was detected for nimesulide, fenofibrate and ibuprofen, they behaved like Class II compounds, i.e crystallized upon heating, after storage (Fig. 3). Further, the ΔC_p at the T_g for these compounds after storage was lower than at time zero (Table 3).

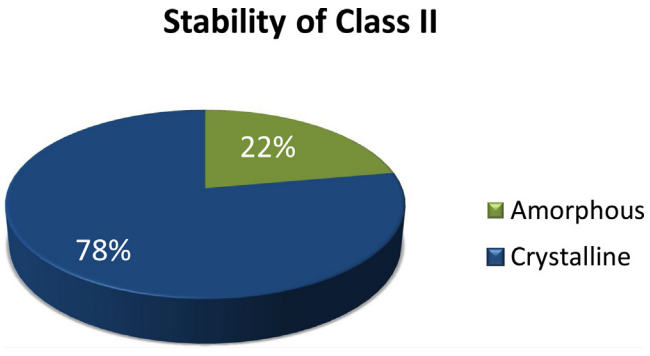

Fig. 1. Stability results for Class II compounds; $n = 18$; stored above the T_g.

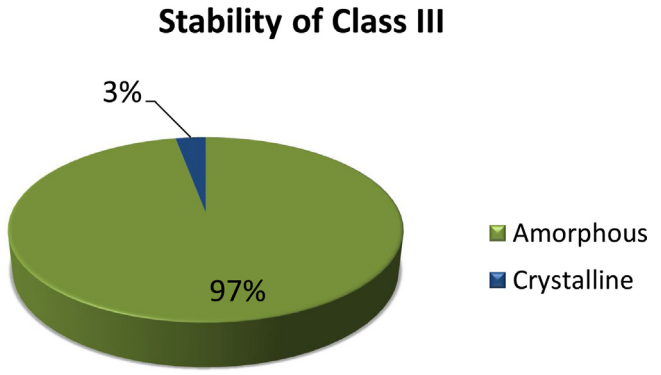

Fig. 2. Stability results for Class III compounds; $n = 34$; stored above the T_g.

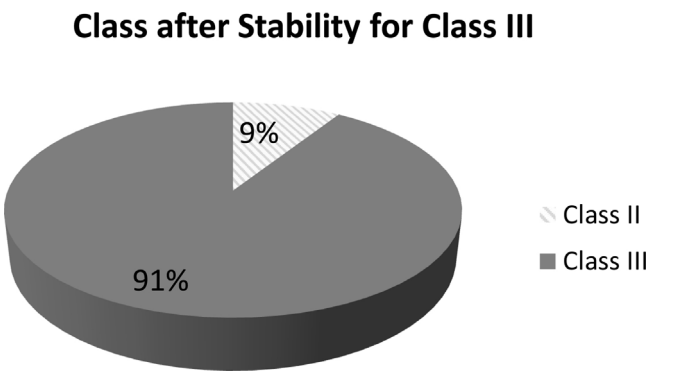

Fig. 3. Stability results for Class III compounds that remained amorphous when stored above the T_g; $n = 33$.

This study indicates that the physical state of the material has a clear effect on the crystallization tendency. This was more pronounced for Class II compounds, which all crystallized when in a supercooled liquid state. Therefore, the storage of amorphous Class II drugs with low T_g values is critical, as the drug will have a high propensity for crystallization.

Fig. 4 shows the relationship between the T_g and the physical stability at temperatures above the T_g. The compounds were investigated under similar conditions and, thus, it is expected that their behaviour will reflect their molecular properties. As can be seen over the range of T_gs, which in this study covers 200 K, some compounds with similar T_gs behaved in opposite ways. The T_g was thus found not to be a factor of importance for the amorphous behaviour and crystallization tendency near the T_g of a compound. However, it was found that it was mainly compounds from Class III that remained amorphous after 12 h at the elevated temperature, while Class II compounds crystallized. Above the T_g, the material is less viscous (more liquid-like) and the molecular mobility is higher, leading to faster crystallization (Kothari et al., 2014; Yoshioka et al., 1994). However, it has been shown that the

Table 3
Heat capacity change at T_g (ΔC_p) (J g °C^{-1}) at time 0 and after 12 h′ storage for Class III compounds that behaved like Class II compounds after storage.

Time (h)	Ibuprofen	Fenofibrate	Nimesulide
0	0.43	0.48	0.50
12	0.43	0.18	0.41

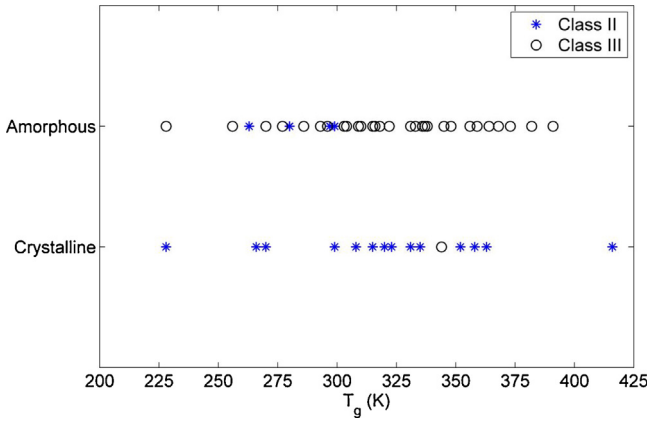

Fig. 4. Relationship between the T_g and the solid-state type (amorphous/crystalline) after the stability study for Class II (blue star) and Class III (black circle) compounds.

molecular properties of the drug have a great impact on its crystallization tendency during storage (Mahlin and Bergström, 2013; Trasi et al., 2014). Molecular descriptors reflecting symmetry, electrotopology, polarizability and molecular size have been used to predict stability, and for instance larger drug molecules typically are less prone to crystallize (Mahlin and Bergström, 2013; Alhalaweh et al., 2014).

The relationship between the tendency to crystallize and the ΔG_v was investigated to discover the extent to which this thermodynamic property is reflected in the classification system (Fig. 5 and Table 1). No clear trend was found, which is in agreement with other findings in the literature (Trasi et al., 2014). However, it has been predicted earlier that the driving force for nucleation increases with increased $\Delta G_{v,,}$, as shown by increased heat of fusion (Bhugra and Pikal, 2008). This relationship did not hold for our data set (Fig. 5).

Our results show that Class II compounds crystallized from supercooled liquid when they were kept for a longer time, while Class III compounds were not affected. This clearly distinguishes the behaviour of Class II drugs from that of Class III drugs. The class II compounds did not crystallize from the glassy state, which demonstrate the impact of the physical state on crystallization as well as the inability to relate the crystallization from a supercooled liquid to that from the glassy state.

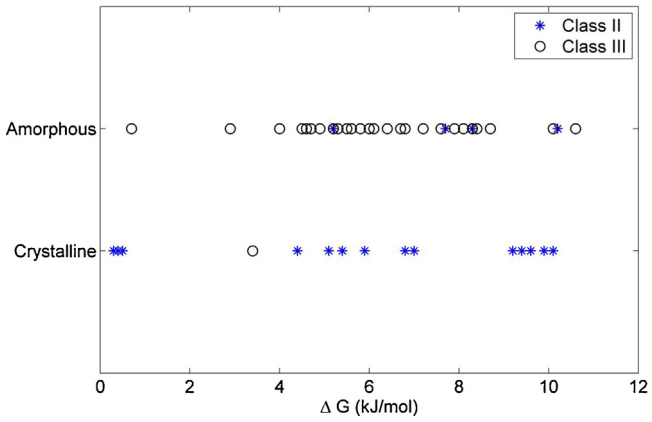

Fig. 5. Relationship between the free energy change and the stability result (amorphous/crystalline) after storage above the T_g for Class II (blue star) and Class III (black circle) compounds.

3.3. Model prediction of physical stability

Computational prediction of drug properties from the molecular properties at an early stage in drug development is of great interest (Alhalaweh et al., 2013, 2014; Alzghoul et al., 2014). Since none of the compounds crystallized below T_g, computational modeling was only done on stability data from studies above the T_g. It was found that the descriptor reflecting the Hückel pi atomic charges for carbon atoms had the lowest p-value (0.02) when the two-sample t-test was performed. Analysis of this descriptor showed that compounds with Hückel pi atomic charge values for carbon atoms greater than 0.5 remain amorphous (17 out of 20) upon storage above the T_g. However, it was not possible to differentiate compounds when this descriptor was less than 0.5. Therefore, other descriptors (i.e. all 280 descriptors except Hückel pi atomic charges for carbon atoms) were gradually added, one at a time, to see if the performance improved. The best performance was seen when the value representing the fraction of aromatic bonds was added to the Hückel pi atomic charges for carbon atoms descriptor. The addition of still more descriptors did not improve the result. Thus, the final SVM model was trained using the whole training data set, represented by these two descriptors, and using a radial basis function (RBF) kernel with sigma = 0.8. The results showed that the proposed SVM-based prediction model was able to correctly classify the stability of the compounds above the T_g for 83% of the training set, and 82% of the test set, as shown in Fig. 6. The good classification accuracy shows that the SVM decision boundary (i.e the red line in Fig. 6) well-separated compounds that were amorphous after the stability study (green circle in Fig. 6) and crystalline after the stability study (blue triangular in Fig. 6). The Hückel and aromaticity parameters affect the molecular conformation, (Alonso et al., 2014; Pulkkinen et al., 2000) and the molecular conformation affects the crystallization of the molecule (Back et al., 2012; Bar and Bernstein, 1987; Bernstein and Hagler, 1978). Compounds with more aromatic bonds seem to crystallize faster at storage conditions above the T_g. Some compounds with high Hückel values are lacking aromatic structures and have a lower crystallization propensity. However, our model identified two important parameters that can classify the tendencies of compounds to crystallize from the supercooled liquid. Other factors that we have identified earlier, such as the molecular

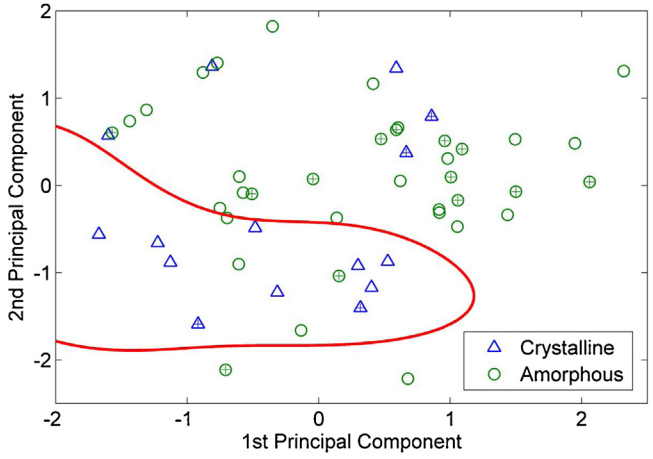

Fig. 6. Prediction of glass stability using the support vector machine algorithm for all the study compounds that were amorphous after the stability study (green circle) and crystalline after the stability study (blue triangular). The crosses indicate the test set. Red line indicates the boundary generated by the SVM model.

weight, size and shape of the molecule, are related to the basic classification of the compounds into Class II or Class III.

These results indicate that the chemical structure of the compound significantly impacts on its crystallization tendencies and can be used, for example, to determine the stability of two compounds with similar T_gs without the need for experimental determination of, for example, the class.

4. Conclusion

This study investigated the crystallization tendency and physical stability upon storage of a series of drugs as a function of temperature. All the compounds were stored at 20 K below and above their T_gs to explore their inherent stability and it was revealed that the GFA can be used to predict the physical stability. It was found that Class III compounds remained amorphous under the studied dry conditions. In contrast, the majority of Class II compounds crystallized when stored at 20 K above the T_g but remained amorphous when stored at 20 K below the T_g. The T_g was poorly correlated to the physical stability under the studied conditions, further strengthening previous indications that molecular properties has a considerable impact on both the GFA and the GS. For Class II compounds, the physical state influenced the crystallization tendency; crystallization was faster from an undercooled liquid state than from a glassy state. The developed computational model predicted the stability of the compounds above T_g well, using two chemical descriptors: Hückel pi atomic charges for carbon atoms and aromaticity. To conclude, this study supports previous findings that the molecular structure of a compound holds key information about the GFA and stability of the amorphous state and can be used to better understand, and also to predict, these complex properties.

Acknowledgements

The Swedish Research Council (Grants 621-2011-2445 and 621-2014-3309) and the European Research Council (Grant 638965) are gratefully acknowledged for financial support for this project. We are grateful to Elisabeth and Alfred Ahlqvist for the post doc grant to Amjad Alhalaweh and to VINNOVA for financial support for Ahmad Alzghoul. We also thank Simulations Plus (Lancaster, CA) for providing the Drug Delivery group at the Department of Pharmacy, Uppsala University, with a reference site license for the software ADMET Predictor.

References

Alhalaweh, A., Alzghoul, A., Kaialy, W., 2013. Data mining of solubility parameters for computational prediction of drug-excipient miscibility. Drug. Dev. Ind. Pharm. 40, p904–909.
Alhalaweh, A., Alzghoul, A., Waseem, K., Denny, M., Bergstrom, C.A.S., 2014. Computational predictions of glass-forming ability and crystallization tendency of drug molecules. Mol. Pharm. 11, 3123–3132.
Alonso, M., Geerlings, P., De Proft, F., 2014. Exploring the structure–aromaticity relationship in Hückel and Möbius N-fused pentaphyrins using DFT. Phys. Chem. Chem. Phys. 16, 14396–14407.
Alzghoul, A., Alhalaweh, A., Mahlin, D., Bergström, C.A., 2014. Experimental and computational prediction of glass transition temperature of drugs. J. Chem. Inf. Model. 54, 3396–3403.
Andronis, V., Zografi, G., 1998. The molecular mobility of supercooled amorphous indomethacin as a function of temperature and relative humidity. Pharm. Res. 15, p835–842.
Angell, C., 1988. Perspective on the glass transition. J. Phys. Chem. Solids 49, p863–871.
Back, K.R., Davey, R.J., Grecu, T., Hunter, C.A., Taylor, L.S., 2012. Molecular conformation and crystallization: the case of ethenzamide. Cryst. Growth Des. 12, 6110–6117.
Baird, J.A., Van Eerdenbrugh, B., Taylor, L.S., 2010. A classification system to assess the crystallization tendency of organic molecules from undercooled melts. J. Pharm. Sci. 99, 3787–3806.
Bar, I., Bernstein, J., 1987. Modification of crystal packing and molecular conformation via systematic substitution. Tetrahedron 43, p1299–1305.
Bernstein, J., Hagler, A., 1978. Conformational polymorphism. The influence of crystal structure on molecular conformation. J. Am. Chem. Soc. 100, p673–681.
Bhugra, C., Pikal, M.J., 2008. Role of thermodynamic, molecular, and kinetic factors in crystallization from the amorphous state. J. Pharm. Sci. 97, p1329–1349.
Graeser, K.A., Patterson, J.E., Zeitler, J.A., Gordon, K.C., Rades, T., 2009. Correlating thermodynamic and kinetic parameters with amorphous stability. Eur. J. Pharm. Sci. 37, 492–498.
Hancock, B.C., Carlson, G.T., Ladipo, D.D., Langdon, B.A., Mullarney, M.P., 2002. Comparison of the mechanical properties of the crystalline and amorphous forms of a drug substance. Int. J. Pharm. 241, p73–85.
Hancock, B.C., Christensen, K., Shamblin, S.L., 1998. Estimating the critical molecular mobility temperature (TK) of amorphous pharmaceuticals. Pharm. Res. 15, 1649–1651.
Hancock, B.C., Parks, M., 2000. What is the true solubility advantage for amorphous pharmaceuticals? Pharm. Res. 17, 397–404.
Hancock, B.C., Shamblin, S.L., Zografi, G., 1995. Molecular mobility of amorphous pharmaceutical solids below their glass transition temperatures. Pharm. Res. 12, 799–806.
Hoffman, J.D., 1958. Thermodynamic driving force in nucleation and growth processes. J. Chem. Phys. 29, p1192–1193.
Kauzmann, W., 1948. The nature of the glassy state and the behavior of liquids at low temperatures. Chem. Rev. 43, 219–256.
Kawakami, K., Harada, T., Miura, K., Yoshihashi, Y., Yonemochi, E., Terada, K., Moriyama, H., 2014. Relationship between crystallization tendencies during cooling from melt and isothermal storage: toward a general understanding of physical stability of pharmaceutical glasses. Mol. Pharm. 11, 1835–1843.
Kothari, K., Ragoonanan, V., Suryanarayanan, R., 2014. Influence of molecular mobility on the physical stability of amorphous pharmaceuticals in the supercooled and glassy states. Mol. Pharm. 11, 3048–3055.
Mahlin, D., Bergström, C.A., 2013. Early drug development predictions of glass-forming ability and physical stability of drugs. Eur. J. Pharm. Sci. 49, 323–332.
Mahlin, D., Ponnambalam, S., Heidarian Höckerfelt, M., Bergström, C.A., 2011. Toward in silico prediction of glass-forming ability from molecular structure alone: a screening tool in early drug development. Mol. Pharm. 8, 498–506.
Marsac, P.J., Konno, H., Taylor, L.S., 2006a. A comparison of the physical stability of amorphous felodipine and nifedipine systems. Pharm. Res. 23, 2306–2316.
Marsac, P.J., Shamblin, S.L., Taylor, L.S., 2006b. Theoretical and practical approaches for prediction of drug–polymer miscibility and solubility. Pharm. Res. 23, 2417–2426.
Nascimento, M.L., Souza, L.A., Ferreira, E.B., Zanotto, E.D., 2005. Can glass stability parameters infer glass forming ability? J. Non-Cryst. Solids 351, 3296–3308.
Pulkkinen, J.T., Laatikainen, R., Ahlgrén, M.J., Peräkylä, M., Vepsäläinen, J.J., 2000. Conformational flexibility and role of aromatic?aromatic interactions in the crystal packing of the coordination compounds of some novel quadridentate Schiff bases. J. Chem. Soc. Perkin Trans. 2, 777–784.
Suykens, J.A., Vandewalle, J., 1999. Least squares support vector machine classifiers. Neural Process. Lett. 9, 293–300.
Trasi, N.S., Baird, J.A., Kestur, U.S., Taylor, L.S., 2014. Factors influencing crystal growth rates from undercooled liquids of pharmaceutical compounds. J. Phys. Chem. B 118, 9974–9982.
Weinberg, M.C., 1994. Glass-forming ability and glass stability in simple systems. J. Non-Cryst. Solids 167, 81–88.
Yoshioka, M., Hancock, B.C., Zografi, G., 1994. Crystallization of indomethacin from the amorphous state below and above its glass transition temperature. J. Pharm. Sci. 83, 1700–1705.
Yu, L., 2001. Amorphous pharmaceutical solids: preparation, characterization and stabilization. Adv. Drug Deliv. Rev. 48, 27–42.
Zhou, D., Zhang, G.G., Law, D., Grant, D.J., Schmitt, E.A., 2002. Physical stability of amorphous pharmaceuticals: importance of configurational thermodynamic quantities and molecular mobility. J. Pharm. Sci. 91, 1863–1872.